Science Advances
AAAS

advances.sciencemag.org/cgi/content/full/6/35/eabb3308/DC1

Supplementary Materials for

Examining metastatic behavior within 3D bioprinted vasculature for the validation of a 3D computational flow model

W. F. Hynes, M. Pepona, C. Robertson, J. Alvarado, K. Dubbin, M. Triplett, J. J. Adorno, A. Randles, M. L. Moya*

*Corresponding author. Email: moya3@llnl.gov

Published 26 August 2020, *Sci. Adv.* **6**, eabb3308 (2020)
DOI: 10.1126/sciadv.abb3308

The PDF file includes:

Figs. S1 to S8
Legends for movies S1 and S2

Other Supplementary Material for this manuscript includes the following:

(available at advances.sciencemag.org/cgi/content/full/6/35/eabb3308/DC1)

Movies S1 and S2

Supplementary Materials:

Figures:

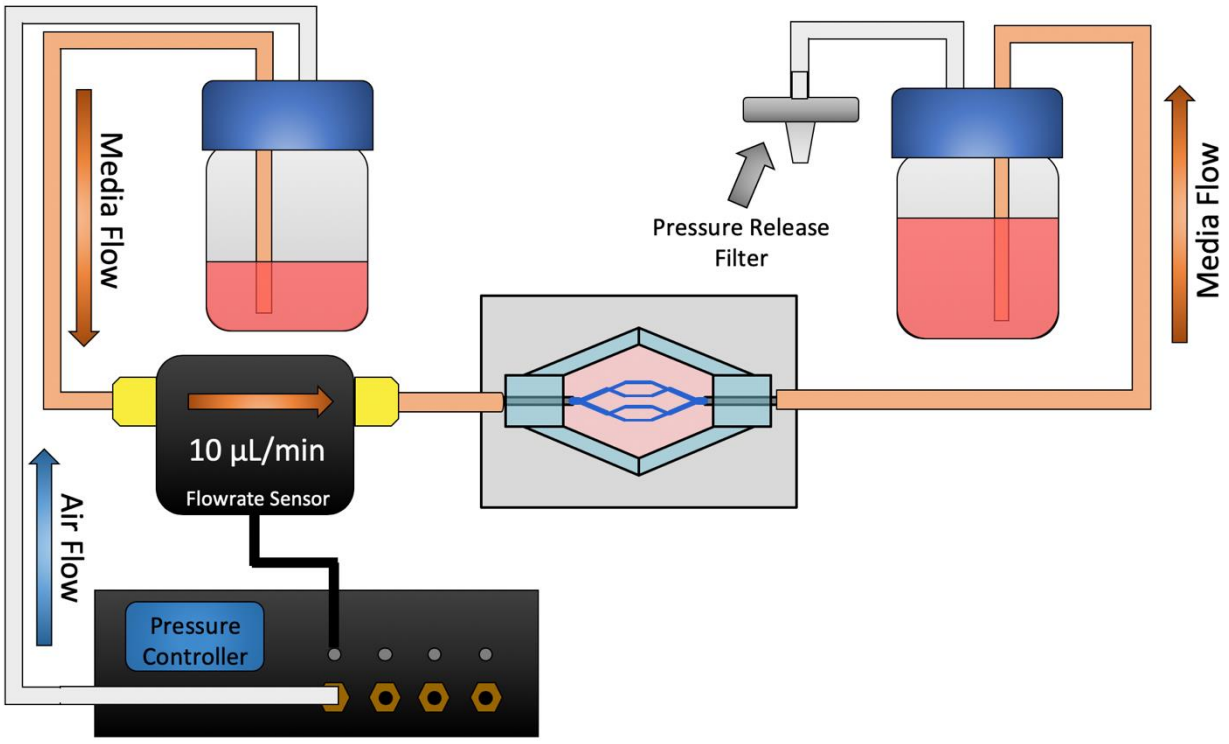

Figure S1: Perfusion Culture Setup. Post-fabrication, vascular bioreactors are connected to a precision pneumatic pumping system to enable continuous perfusion of culture media for the duration of culture. Media is driven from the entry reservoir via pressurization with sterile air, passing through a flow rate sensor which simultaneously measures and regulates the pumping system to maintain a predetermined flow rate. After passing through the sensor, media is pumped through the printed vasculature before being collected in an exit reservoir. The exit reservoir is vented to atmosphere via an air filter, both preventing pressure build-up and allowing the media within to equilibrate to the incubator atmosphere.

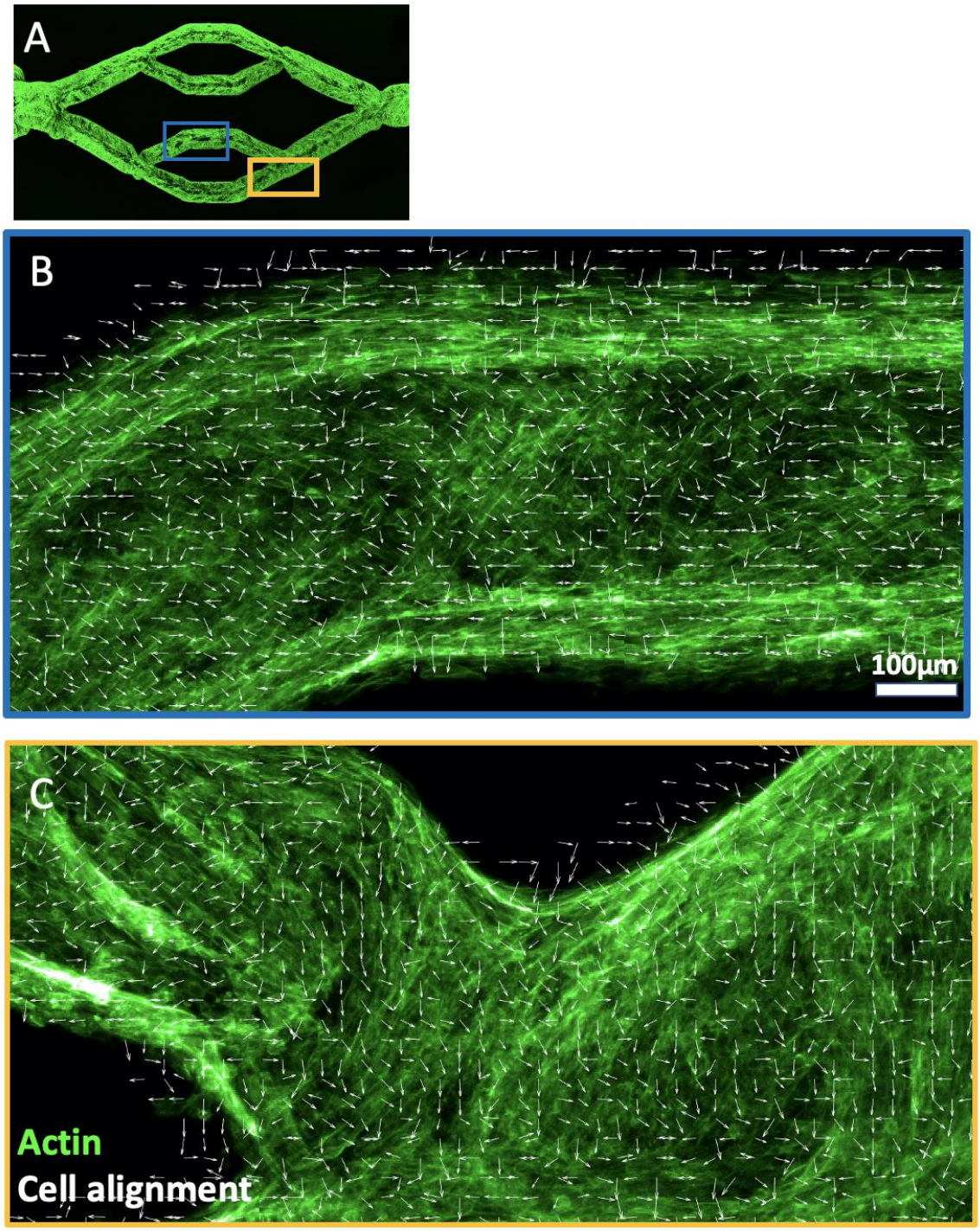

Figure S2: Alignment of endothelial cells in engineered vessels. A: Overview of analyzed regions. **B:** Quiver plots of endothelial cell alignment curved-to-straight transition vessel region shows strong alignment along vascular walls and some alignment along the bottom of the vessel. **C:** An incoming fork shows comparatively disordered alignment.

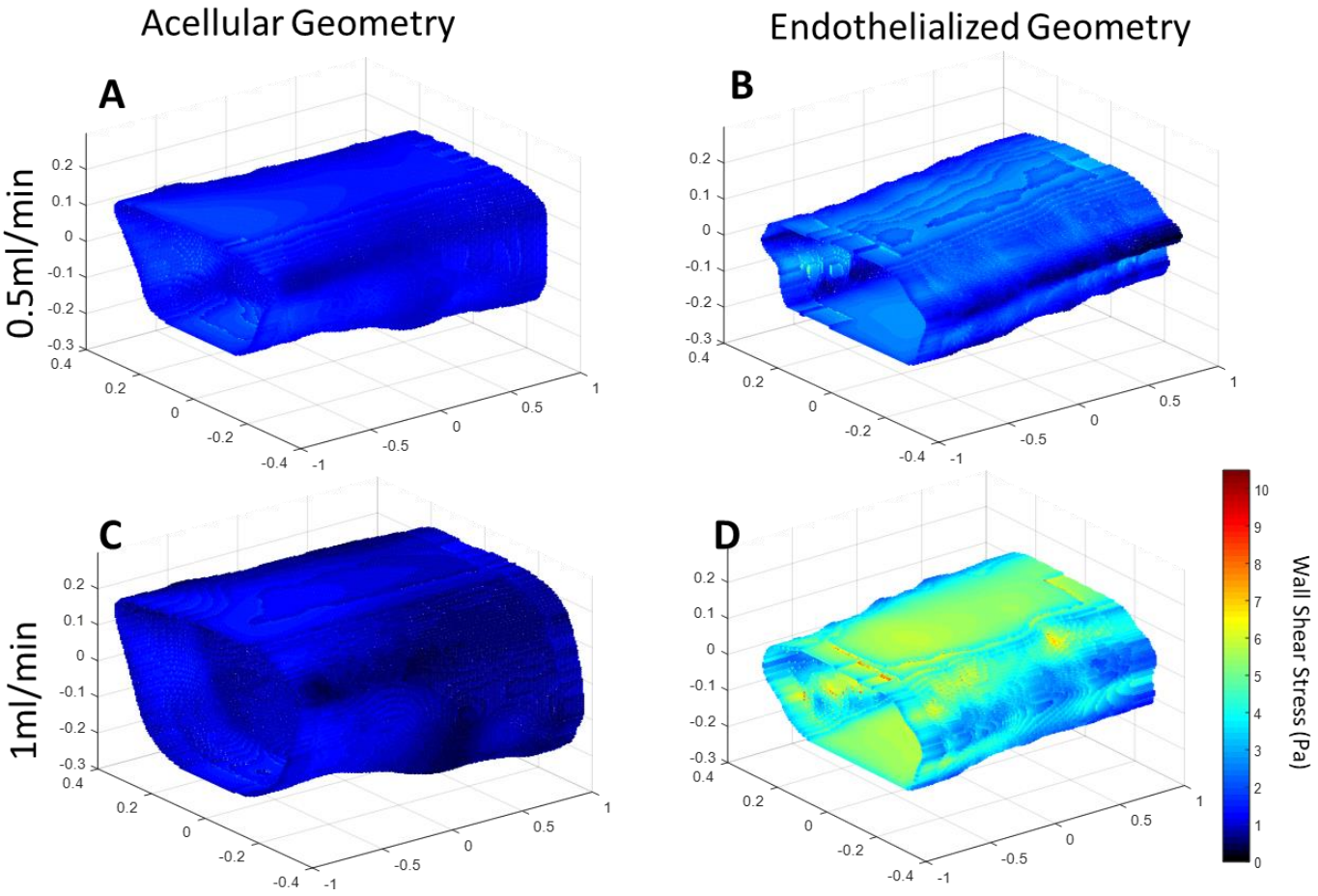

Figure S3: Wall Shear Stress Distributions. A&C: Acellular vessel at 0.5 and 1ml/min shows a decrease in mean wall shear stress, whereas **B&D** the Endothelialized vessel shows marked increase in wall shear stress

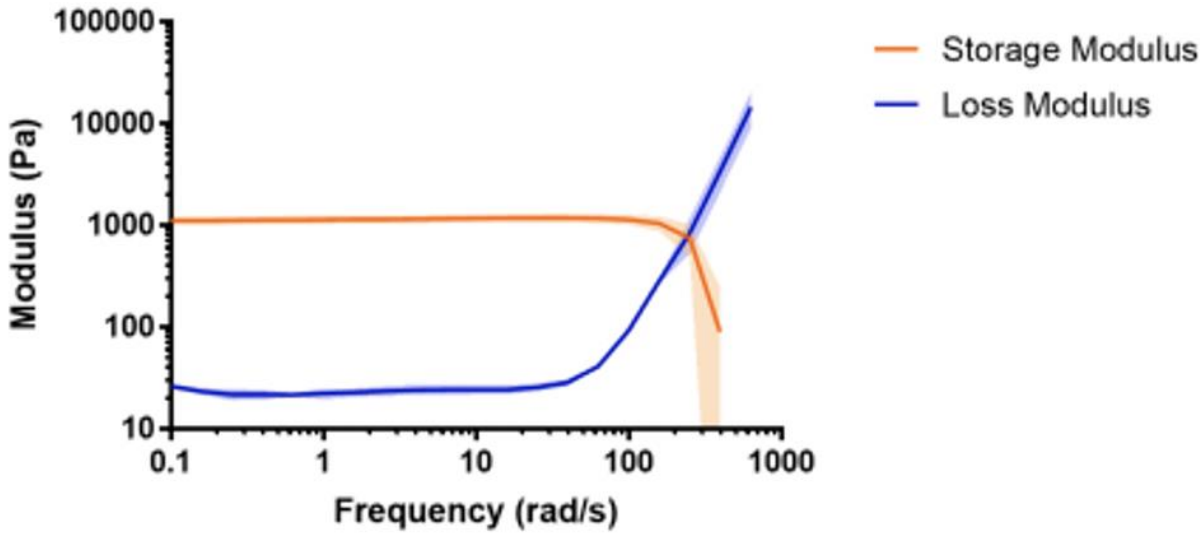

Figure S4: Rheological characterization of ECM hydrogel. Frequency sweep testing on acellular hydrogel samples gelled for 24 hours shows that the hydrogel used for bioprinting is a relatively stiff material with a relatively low loss modulus except at high frequencies.

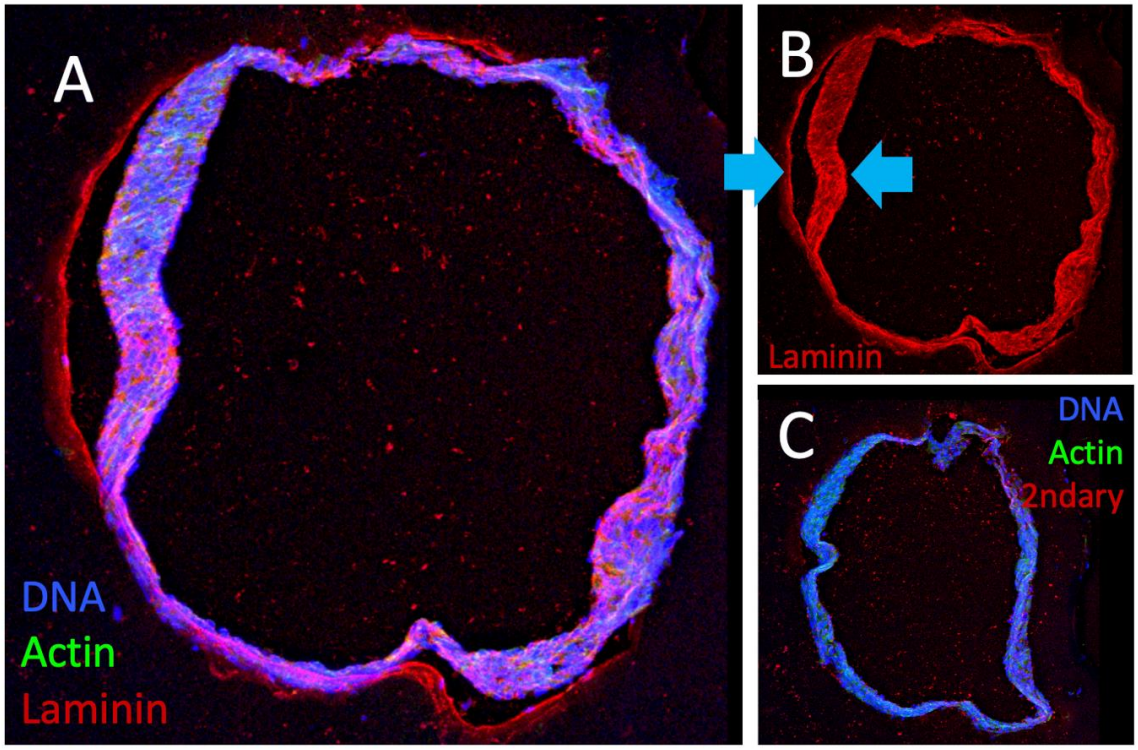

Figure S5: Endothelial cells secrete basement membrane proteins. **A:** Staining for laminin (red) and the actin cytoskeleton (green) demonstrate that endothelial cells secreted laminin. **B:** Both cells and the surrounding ECM show strong staining for laminin. Blue arrows indicate a delamination of cells from ECM during cryosectioning showing laminin in both cell bodies (right arrow) and ECM (left arrow). **C:** Secondary antibody control confirms labeling observed is due only to binding of secondary antibody to the primary.

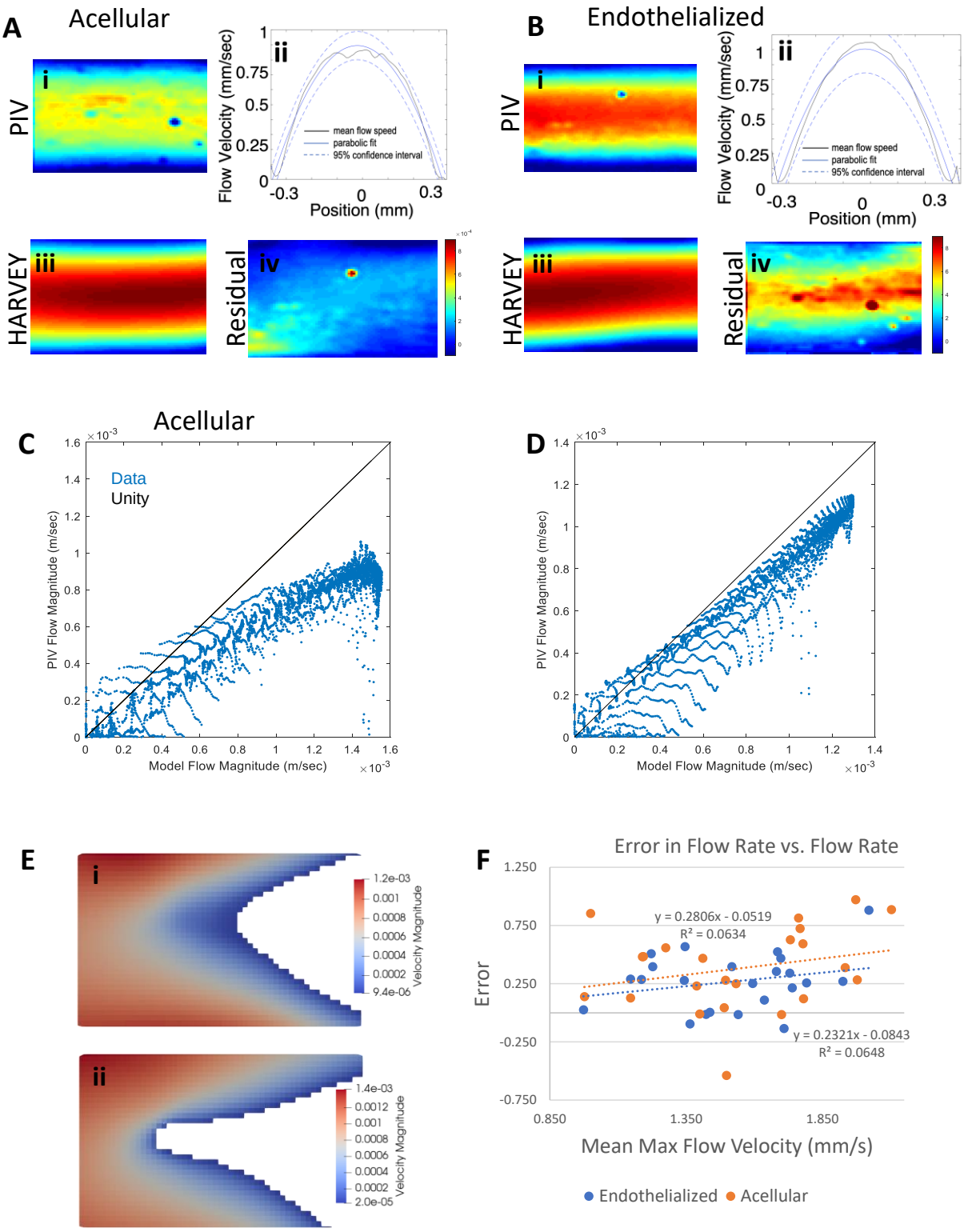

Figure S6: Sources of error in flow patterns. **A&B:** Direct comparison of **i**. flow velocity magnitude measured with PIV to **iii**. flow simulations with HARVEY for a narrow straight channel (Region G in Fig 3E). **ii**. A parabolic flow profile was observed with PIV, and **iv** the residual error

of simulated minus observed shows highest error in the center of the channel where velocity is the highest. **C&D**: Plotting modeled flow rate against observed flow rate reveals blunting at high speeds. **E**: One potential source of error was uncertainty in choice of vertical position in the channel corresponding to PIV measurement. Simulations show a ~20% error in max flow rate when comparing **i**: the vertical center of the channel to a third of the channel height down. **F**: Bland-Altman plotting of experimental flow rate error when compared to simulated results between locations within the endothelialized and acellular branching vessels shows that error goes up with max flow velocity.

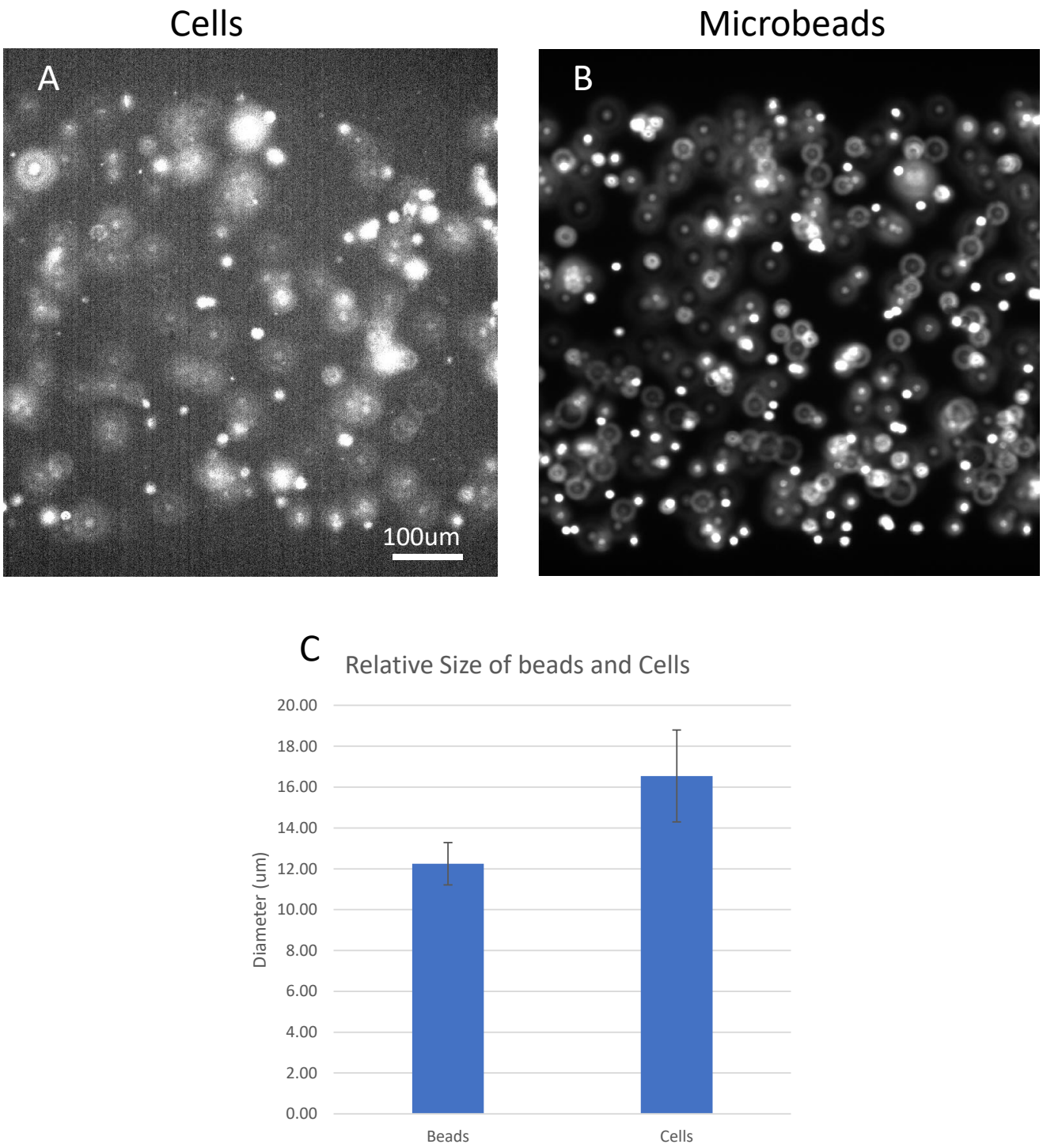

Supplemental Figure S7: Relative size distribution for **(A)** 4T1 mammary carcinoma cells and **(B)** polystyrene microbeads shows **(C)** small differences in observed sizes

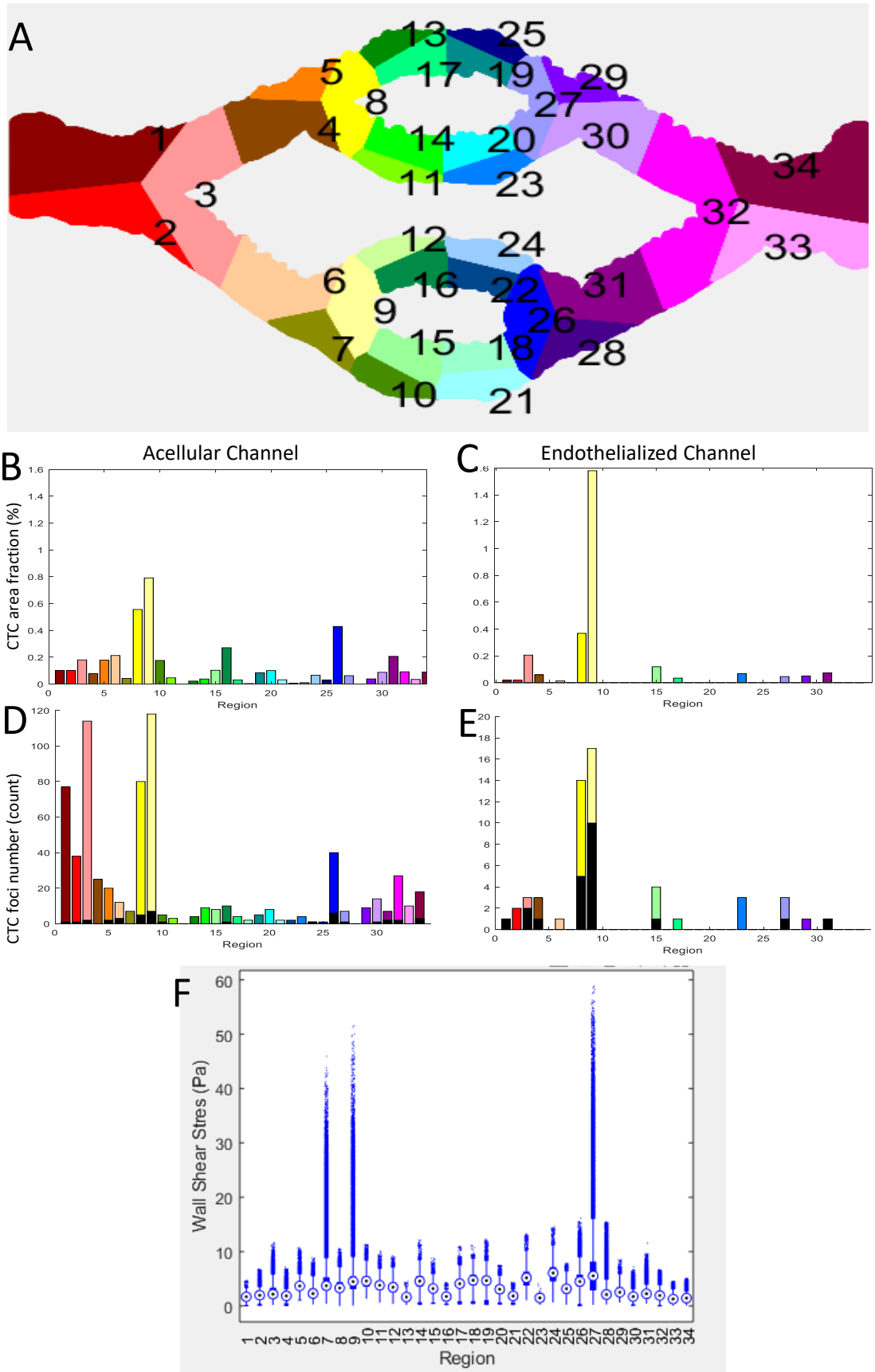

Figure S8: Attached CTCs by region: A: Curvature change points were identified and used to divide the vessel geometry into regions. CTC number and area were counted for each region for both the **B&D**

acellular and **C&E** endothelialized regions. The incoming fork regions (3,8 and 9) were especially susceptible to CTC attachment. A higher CTC area fraction was observed in the acellular channel, and much higher numbers of CTC foci were detected, but number of large CTC foci was higher in the endothelialized incoming forks. **F:** Whisker plot comparing wall shear stresses present at all regions delineated in **(A)** within the endothelialized device gathered from $13x10^6$ total data points originating from HARVEY simulation.

Movies

Movie S1: Flow of deformable cells (Gs = 10-5 N/m) in the scaled straight channel.

Movie S2: Flow of idealized rigid, spherical particles (Gs = 10-3 N/m) in the scaled straight channel.